94-237

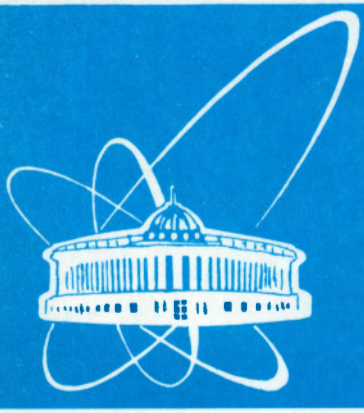

объединенный
институт
ядерных
исследований
дубна

E9-94-237

E.L. Saldin*, V.P.Sarantsev, E.A.Schneidmiller*,
Yu.N.Ulyanov*, M.V.Yurkov

FREE ELECTRON LASER AS ENERGY DRIVER FOR INERTIAL CONFINEMENT FUSION

Submitted to «Nuclear Instruments and Methods A»

*Automatic Systems Corporation, Smyshlyaevskoe Shosse 1a, 443050 Samara, Russia

1994

1 Introduction

One of the possible ways to solve the problem of controlled thermonuclear synthesis is application of inertial confinement fusion (ICF), when thermonuclear fuel is exploded under shocking action of laser radiation. The key problem of such an approach is that of a laser. Several severe requirements are imposed on the laser system parameters. To provide sufficient compression and heating of the target, total energy of laser flash should not be less than 1 MJ. This energy should be fed to the target within a pulse with definite temporal characteristics and duration about of 0.1 – 1 nanoseconds. To provide effective focusing of radiation at the target, the laser system should possess a high brightness. Thermonuclear target should be radiated symmetrically with respect to its center via several tens of directions. Laser light wavelength should be less than 0.6 μm. At a longer wavelength, absorption of energy in the target becomes ineffective due to reflections from the surface plasma layer. Finally, to construct commercial reactor, the laser efficiency should be greater than 5 per cent and repetition rate should be several cycles per second.

Nowadays the approach to construct ICF reactor has passed its way of scientific verification in many locations [1]. Unique laser systems based on solid-state Nd lasers have been developed. Experiments have confirmed validity of the approach, densities in excess of 600 times the solid state phase have been reached [2]. Although Nd lasers have served a good role during fundamental experiments on inertial confinement fusion, the problem of optimal choice of the energy driver for ICF commercial reactor is still open. As for solid-state Nd lasers, they possess several significant disadvantages. The main of them are those of cooling the solid-state active medium, of a low efficiency (which is of the order of fraction of per cent) and of a low level of reliability. These impose a limit on the frequency of laser flashes. For instance, the laser NOVA at Livermore performs only several shots per a day. Perspectives of this approach for constructing the ICF energy driver may be connected with the use of the laser diode pumped solid state lasers [3]. Another approach to construct the ICF energy driver assumes to use high power ion beams. A lot of work should be done to prove a validity of such an approach.

During last decade significant achievements have been obtained in the field of free electron laser (FEL) physics and technique. FEL devices possess many attractive features. FEL radiation is coherent and it always has ideal, i.e. diffraction dispersion. Tunability of FEL radiation provides a possibility to vary wavelength in a wide range. FELs are capable to provide a high efficiency of transformation of the electron beam power into the radiation power. It has been demonstrated experimentally, the efficiency of an FEL amplifier has reached the value of 34 % [4]. Remembering that accelerators, providing driving beams for the FELs can provide effective transformation of electric power into the electron beam power, one can expect to reach a high level of the total FEL efficiency. Finally, repetition rate of electron accelerators is rather high, up to several hundreds cycles per second. All these features of the FEL indicate that it should be studied as a candidate on a role of the laser for the ICF commercial reactor.

For the first time a possibility to use the FEL as an energy driver for commercial ICF reactor was considered in ref. [5]. The authors of this paper obtained that direct use of the FEL as a driver requires a power of more than 10^{14} W. So, the total e-beam power should reach astronomical values in that case. As a result, they have proposed to use the FEL for pumping a solid-state laser which has been developed as the fusion driver.

Contrary to the conclusion of the paper [5], our investigation has led us to an optimistic conclusion that construction of the FEL system meeting the requirements to the ICF energy driver is quite possible at the present day level of accelerator technique R&D. It becomes possible due to application of a novel FEL amplifier scheme proposed in our paper. In this scheme the required level of the output power is provided by the use of summing the optical power technique. This technique operates as follows. Multi-stage FEL amplifier is composed of a large number N of undulators separated with magnetic snakes. The FEL driving electron beam is generated by a linear RF accelerator which produces a train of N electron bunches. This train is fed into entrance of the first stage FEL amplifier together with the single optical pulse of the master oscillator which is synchronized with the last electron bunch of the train. In the first stage of the FEL amplifier the optical pulse is amplified taking the energy off the last electron bunch. After passing the first undulator, the optical and electron bunches are separated in the magnetic snake: the train of electron bunches moves along the curved trajectory between the undulators, while the optical beam travels along the straight line. Parameters of the snakes are chosen in such a way that the difference of paths of electron and optical bunch is equal to the distance between the electron bunches, so, at the entrance to the next FEL amplifier stage, the optical bunch is synchronized with the next, unperturbed bunch of the train, etc. Parameters of the undulator of each stage are optimized on effective extraction of the energy off the electrons, taking into account the growth of the optical power. As a result, this scheme provides a benefit in a peak radiation power of the order of N, the number of the FEL amplifier stages, and the peak radiation power can be done much more than the peak power of electron beam.

It should be noticed that the FEL amplifier has rather large length, and radiation field gain is relatively small in the most number of the FEL amplifier stages, so the self-focusing of radiation (or effect of "optical guiding" [6]) can not provide effective focusing of radiation. The next problem to be solved is the problem of effective focusing system with low losses and stable to the action of the powerful laser radiation.

Объединенный институт ядерных исследований БИБЛИОТЕКА

In the presented paper we propose to use a periodic diaphragm line for focusing the radiation. It has a form of a sequence of totally absorbing screens with holes. When Fresnel number is large, eigenmodes of diaphragm line have rather small diffraction losses. For instance, in a visible wavelength range, at the radius of the hole 1 cm and the distance between the screens 1 m, diffraction losses of the ground eigenmode are about of 0.01 % per one diaphragm. So, the use of the diaphragm focusing line is the second basic idea of the paper.

Using these basic ideas, we have developed conceptual project of the ICF driver on the base of multichannel multi-stage FEL amplifier. The FEL driving electron beam is produced by 3 GeV linear accelerator operating at frequency 500 MHz with pulse duration 25.6 μs and repetition rate 40 Hz. Micropulse duration is equal to 100 ps and peak current is equal 2 kA. Total number of electron bunches in a macropulse is equal to 6400 with the energy store equal to 3.84 MJ. FEL amplifier consists of 64 parallel channels. A system of kicker magnets separates electron bunches via 64 FEL amplifier channels. Each FEL amplifier channel is a multi-stage amplifier with 90 stages. At the exit of the amplifier, total energy of laser flash is equal to 1 MJ with a brightness 4×10^{22} W cm^{-2} sr^{-1}. Total efficiency of the proposed energy driver is about of 11 %.

Linear dimensions of the FEL based ICF driver are about of 5 km and are comparable with those of the ion beams based ICF driver (see, for instance, ref. [7]), while the problems of technical realization can be solved at the present level of accelerator technique R&D.

The paper proceeds as follows. In sections 2 and 3 we describe briefly basic ideas of the proposal, namely the summation scheme of the optical power and use of diaphragm line for focusing and transporting optical radiation. Section 4 presents a conceptual project of the FEL based ICF energy driver. Section 5 is devoted to the problems of optimal choice of the multi-stage FEL amplifier. In Section 6 we discuss problems of technical realization of the proposed energy driver.

2 Summation of optical power

In traditional scheme of the FEL amplifier, output radiation power W_{opt} does not exceed the electron beam power W_e,

$$W_{opt} = \eta_{FEL} \times W_e = \eta_{FEL} \times I_{peak} \times \mathcal{E}/e,$$

where η_{FEL} is the FEL amplifier efficiency ($\eta_{FEL} < 1$), I_{peak} and $\mathcal{E}$ are the peak current and the energy of electron beam, respectively. The peak power of the energy driver for inertial confinement fusion should be of the order of several thousands of terawatts which

results in enormous values of the electron beam parameters. On the other hand, the present level of accelerator technique R&D allows one to construct accelerators with the energy about of several GeV and peak current about of several kA with sufficiently low energy spread and emittance. So, it seems to be unreal to overcome a TW level of the FEL output power using standard approach.

To overcome this problem, we propose to use multi-stage FEL amplifier which amplifies a single optical bunch by means of sequential usage of several electron bunches. FEL amplifier is composed of a large number N_s of undulators separated with magnetic snakes (see Fig.1).

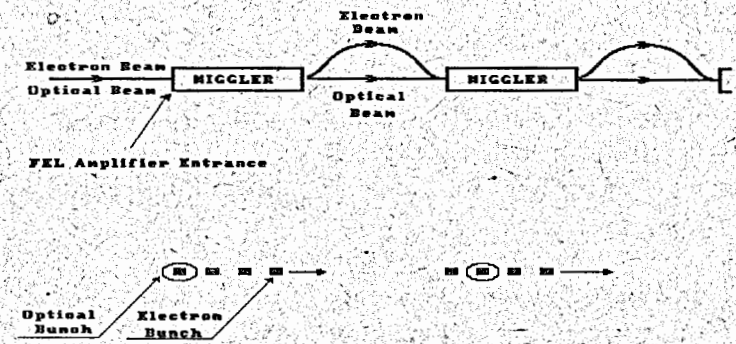

Figure 1: The scheme of optical power summation

The FEL driving electron beam is generated by a linear RF accelerator which produces a train of N_s electron bunches. This train is fed into entrance of the first stage of the FEL amplifier together with the single optical pulse of the master oscillator which is synchronized with the last electron bunch of the train. In the first stage of the FEL amplifier the optical pulse is amplified taking the energy off the last electron bunch. After passing the first undulator, the optical and electron bunches are separated in the magnetic snake: the train of electron bunches moves along the curved trajectory between the undulators, while the optical beam travels along the straight line. Parameters of the snakes are chosen in such a way that the difference of paths of electron and optical bunch is equal to the distance between the electron bunches, so, at the entrance to the next FEL amplifier stage, the optical bunch is synchronized with the next, unperturbed bunch of the train, etc. Parameters of the undulator of each stage are optimized on effective energy extraction off the electrons, taking into account the growth of the optical power. As a result, this scheme provides a benefit in the peak radiation power of the order of N_s, the number of the FEL amplifier stages, and the peak radiation power can be done much more than the peak power of electron beam.

The optical power summation scheme, described above, does not exhaust all the possible configurations of summation schemes. They may be realized also by providing the delay of optical bunch with respect to electron bunches by means of optical delay lines (in this case the optical bunch is synchronized with the first electron bunch of the train at the first FEL amplifier stage).

This scheme may be used also with the driving beam from the linear induction accelerator (LIA). As a rule, the LIA electron beam has a rather long duration T_b, about of several tens or hundreds of nanoseconds. To amplify a short optical beam with duration $T_{opt} \ll T_b$, one may construct multi-stage FEL amplifier with the number of stages equal to $N_s = T_b/T_{opt}$. At the entrance into the first stage, the optical beam should be synchronized with the tail of electron beam and delay lines should provide a shift between the optical and electron bunches by the value of the optical pulse duration T_{opt}.

This scheme operates successfully when the master laser signal significantly exceeds the value of the noise signal in the first FEL amplifier stage. For the parameters of the numerical example presented in this paper, the power of the FEL amplifier noise is of the order of $< W_{sh} > \simeq 40$ W (see section 5.1), while the master laser power is about of 1 MW.

In the multi-stage FEL amplifier there may appear a transportation problem of used electron bunches in the magnetic system of subsequent FEL amplifier stages, because there is significant energy spread in these bunches. To avoid this problem, a high dispersion may be realized in the magnetic snakes which provides separation of the electrons in space by their energy. Then the electrons, which energy differ significantly from the nominal one, may be absorbed by beam dumps.

3 Diaphragm focusing line

As a rule, lens systems are used for transporting and focusing of optical radiation. While this technique is appropriate at a relatively small radiation power, it is completely unfit for focusing and transporting of powerful laser beams with the average and peak radiation power about of one megawatt and several hundreds terawatts, respectively. Nevertheless, this problem may be solved by using diaphragm focusing line which has a form of periodically spaced screens with holes. For an axisymmetric line with the period L, eigenfunctions $\Phi_m(r,\varphi)$ have the form:

$$\Phi_m = u_{mj}(r)\exp(-\mathrm{i}m\varphi), \qquad m = 0,1,2,\ldots \tag{1}$$

When radius of the holes R is rather large, $R \gg \lambda$, in the first order of a small parameter $M = (8\pi N_F)^{-1/2}$, where $N_F = R^2/(\lambda L)$ is Fresnel number, functions u_{mj} have the form [8]:

$$u_{mj} = J_m(k_{mj}r), \tag{2}$$

where $k_{mj} = \mu_{mj}(1-\Delta_0)/R$, $\Delta_0 = (1+i)\beta_0 M$, $\beta_0 = 0.824$, μ_{mj} is j-th root of the Bessel function of the m-th order (i.e. $J_m(\mu_{mj}) = 0$). For TEM_{mj} eigenmode, a fraction of the radiation power losses per passage of one diaphragm is given with the relation:

$$\Delta W_{rad}/W_{rad} = 8\mu_{mj}^2 M^3 \beta_0. \tag{3}$$

When Fresnel number N_F is large, eigenmodes of diaphragm line have rather small diffraction losses. For instance, in a visible wavelength range, at the radius of the hole $R \sim 1$ cm and the distance between the screens $l \sim 1$ m, diffraction losses of the ground TEM_{00} eigenmode are about of 0.01 % per one diaphragm.

Diaphragm line is rather stable with respect to misalignment of the screens. When the screens are adjusted in the both transverse and longitudinal directions with the accuracy about of 10^{-2} cm (which is usual in the accelerator technique), misalignments do not result in the extra diffraction losses (see Appendix A for more details).

4 Conceptual project of the FEL based ICF energy driver

In the present paper we do not touch the problems of the general ICF reactor design. We assume the ICF reactor to be designed on the base of standard scheme when thermonuclear fuel is exploded in a reactor chamber under shocking action of laser radiation and heats the walls of the reactor chamber. Then the heat is transformed into electrical power by standard technique (see, for instance, ref. [9] and references therein). Experimental and theoretical researches have shown that construction of such a reactor becomes feasible when the laser system possesses the following parameters: energy of laser flash $\gtrsim 1$ MJ within steering pulse duration, repetition rate $\gtrsim 10$ cycles per second and laser efficiency $\sim 5-10$ % [9]. In this paper we analyze only a possibility to construct such a laser system using FEL technique.

General parameters of the FEL based ICF energy driver are presented in Table 1. Its key elements are high-current RF linear accelerator, separation system and multi-channel, multi-stage FEL amplifier.

Driving electron beam for the FEL amplifier is generated by linear Rf accelerator. It operates at 40 Hz frequency and generates trains of 6400 electron bunches with total stored energy 3850 kJ. Then this train of electron bunches is separated by separation system into 64 trains of bunches which are fed into entrances of 64 parallel multi-stage FEL amplifier channels. Each FEL amplifier channel is a multi-stage FEL amplifier with

Table 1: ICF driver parameters

Wavelength λ, μm	0.5
Laser pulse length, ns	0.1 – 2
Laser beam brightness, W/cm^2	4×10^{22}
Total number of channels	64
Total number of stage in channel	90
Energy / pulse, MJ	1
Repetition rate, Hz	40
Efficiency, %	11

90 stages. At the exit of the amplifier, total energy of laser flash is equal to 1 MJ with a brightness 4×10^{22} W cm^{-2} sr^{-1}.

4.1 High-current RF accelerator

Driving electron beam for the FEL amplifier is generated by linear RF accelerator (see Table 2). Accelerating structure consists of separated cavities and each cavity is fed by separate klystron (see Fig.2).

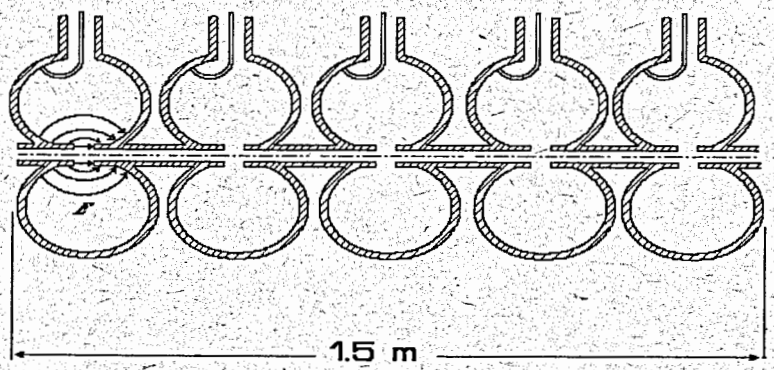

Figure 2: Accelerating structure

RF accelerating wavelength is chosen to be rather large, $\lambda_{rf} = 60$ cm, which is connected with a high beam loading. Accelerating gradient is equal to 2 MV/m and total length

Table 2: Accelerator parameters

Electron energy $\mathcal{E}_0$, GeV	3
Beam peak current I, kA	2
Micropulse duration, ps	100
Bunch spacing, ns	4
Macropulse duration, μs	25.6
Energy spread σ_E/E, %	0.1
Normalized emittance ϵ_n, cm·rad	3×10^{-3}
RF frequency, MHz	500
Accelerating Gradient, MV/m	2
Length of accelerator, m	1500
Shunt impedance, MΩ/m	8
Stored RF energy, J/m	3.7
Q-factor of unloaded structure	2.5×10^4
Q-factor of loaded structure	1.2×10^2
Wall power losses, kW/m	450
Repetition rate, Hz	40

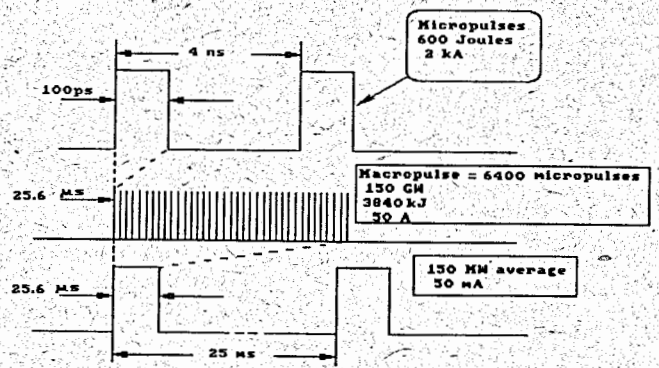

Figure 3: Electron beam pulse format

of accelerator is equal to 1500 m. Accelerator operates at repetition rate 40 Hz. During one macropulse ($\tau = 25.6$ μs), the accelerator produces a train of 6400 electron bunches

(I_{peak} = 2 kA, τ = 100 ps, $\mathcal{E}$ = 3 GeV) with total stored energy 3850 kJ (see Fig.3). Averaged over macropulse current is equal to 50 A.

Total RF power losses in one cavity are equal to 33 MW (including 150 kW of heat losses).

Total efficiency of the accelerator η_{ACC} (i.e. efficiency of electrical power conversion into the electron beam power) is given by,

$$\eta_{ACC} = \eta(\mathrm{rf} \rightarrow e) \times \eta(\mathrm{klystron}) \times \eta(\mathrm{modulator}), \qquad (4)$$

where $\eta(\mathrm{rf} \rightarrow e)$ is the efficiency of RF power conversion into the electron beam power, η(klystron) is the klystron efficiency and η(modulator) is the efficiency of klystron modulator. So as the peak accelerated current is rather high and RF pulse duration is much more than filling time of the loaded structure, the efficiency of the RF power conversion $\eta(\mathrm{rf} \rightarrow e)$ into the electron beam power is rather large, $\eta(\mathrm{rf} \rightarrow e) \simeq 0.99$. It is rather realistic to assume the efficiency of the modulator to be equal to $\eta(\mathrm{modulator}) = 0.8$. Assuming the klystron efficiency to be $\eta(\mathrm{klystron}) = 0.5$, we obtain the total efficiency of the accelerator to be equal to $\eta_{ACC} = 0.4$.

4.2 Separation system

The train of 6400 electron bunches from the driving accelerator, spaced by 4 ns, is separated into 64 trains of 90 bunches to be fed into entrances of 64 parallel multi-stage FEL amplifier channels. Separation of electron bunches is performed by kicker magnets using sequential scheme (see Fig.4). In this scheme, after k-th stage, there are 2^k parallel channels with 2^k trains of bunches in each. At $(k+1)$-th stage, each of 2^k channels is separated into two channels, i.e. each train is divided by a half and each half-train is directed into separate channel. Thus, such a scheme consists of 6 stages ($2^6 = 64$) and 63 kicker magnets ($2^6 - 1 = 63$). Simultaneous arrival of all trains to the FEL amplifier entrances is provided by using different lengths of channels.

Pulse duration of the kicker magnets depends on their place in the separation system and are equal to 12.8 μs, 6.4 μs, 3.2 μs, 1.6 μs, 0.8 μs and 0.4 μs for the 1st, 2nd, 3rd, 4th, 5th and 6th stages, respectively. So as each kicker magnet deflects only a half of a train, it is necessary to minimize only a rise or fall time of the kicker magnets. At the value of rise (fall) time about of 50 ns, about of 10 bunches are lost per separation stage which results in the efficiency of separation system to be $\eta_{SEP} = 0.9$. As a result, separation system provides transporting the trains of 90 bunches to each of 64 FEL amplifier channels.

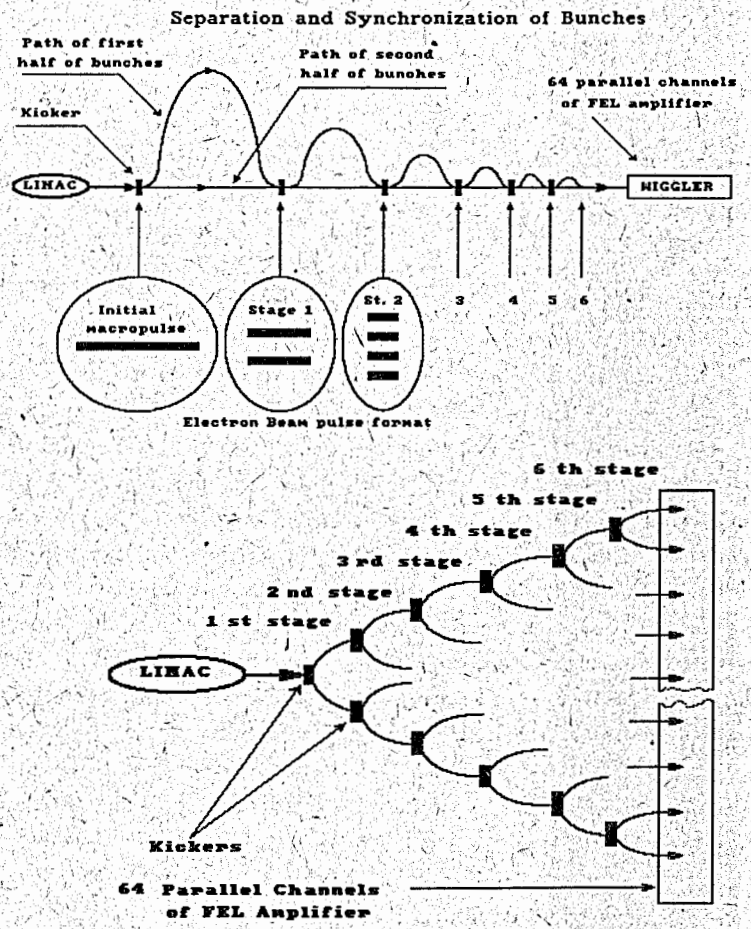

Figure 4: Separation and synchronization of bunches

4.3 Multi-channel FEL amplifier

FEL amplifier consists of 64 separate channels and each of them is multi-stage FEL amplifier providing amplification of a single optical pulse. Each multi-stage FEL amplifier is composed of 90 undulators separated with magnetic snakes. The train of 90 electron bunches is fed into entrance of the first stage of the FEL amplifier together with the single optical pulse of the master oscillator which is synchronized with the last electron bunch of the train. Then the optical beam is amplified using optical power summation scheme (see section 2). Parameters of the undulator of each stage are optimized on effective extraction of the energy off the electrons, taking into account the growth of the optical power from one stage to another. Assuming average efficiency of each amplifier stage to be $\eta_{FEL} = 0.3$, we obtain that the energy of each optical pulse at the amplifier exit is much more than the energy of single electron bunch and is equal to 16 kJ. 64 FEL amplifier channels provide total energy of optical flash to be equal to 1 MJ.

The first stage of the FEL amplifier is destined to amplify relatively weak signal from the master laser ($W_{ext} \simeq 1$MW) by a factor of the order of 10^5. It is designed by a standard way, i.e. its undulator has a long untapered section and a section with tapered parameters (see section 5.1). Output radiation power at the exit of the first stage is of the order of the electron beam power. Subsequent stages of the FEL amplifier amplify a powerful optical beam and provide small amplification per one stage. They operate in a tapered regime from the very beginning and are designed using a scheme of multicomponent undulator (i.e., prebuncher – dispersion section – tapered undulator). To provide effective focusing of the radiation in these FEL amplifier stages, the diaphragm focusing line is used (see section 5.2 and Appendix B for more details).

Total length of the 90 stages of the FEL magnetic system is equal to 5500 m (including 900 m of the lengths of magnetic snakes).

Quality of optical beam

Parameters of radiation of the proposed FEL system meet all the requirements to the ICF energy driver.

First, there is no significant preheat of the target. The radiation power, fed to the target prior arrival of the main pulse, is defined mainly by the superradiation of the electron bunches in the first stage of the FEL amplifier. Undulator of this stage has a long untapered section which provides exponential amplification of a signal by 10^4 times. It will be shown in section 5.1 that the amplitude of effective shot noise at the FEL entrance is about of 40 W. All the electron bunches of the train, with except of the last, generate optical radiation with the power about of 4×10^5 W. This effect does not takes

place in the subsequent stages of the FEL amplifier, because undulators of these stages are manufactured with a deep tapering. So, during time period about of 1 μs until the arrival of the main pulse with the energy 1 MJ, the target will receive the energy about of 10^{-1} J. As a result, contrast of the FEL based ICF energy driver is larger than 10^7.

Second, a form of the optical pulse influences significantly on the process of the target implosion. The proposed scheme provides wide possibilities to steer the optical pulse form and duration. It may be done, for instance, by introducing separate delays of electron trains in different FEL amplifier channels.

Third, to provide effective focusing of radiation on the target, the laser should provide a high brightness B_l:

$$B_l = W_{opt}/(S\pi\alpha^2),$$

where W_{opt} is the peak laser power, S and α are the square and the angle divergence of the radiation at the laser exit, respectively. An ultimate brightness of powerful solid-state laser systems does not exceed the value of 10^{19} W/(cm^2·sr). We have emphasized above the radiation of the FEL amplifier always has minimal, i.e. diffraction dispersion. Using data from Table 1, we obtain that the FEL based ICF energy driver possesses the brightness $B_l = 4 \times 10^{22}$ W/(cm^2·sr).

4.4 Efficiency of the ICF reactor

The efficiency of the proposed ICF energy driver is given by

$$\eta_{TOT} = \eta_{ACC} \times \eta_{SEP} \times \eta_{FEL}. \qquad (5)$$

Assuming the efficiency of the accelerator η_{ACC}, of the separation system η_{SEP} and of the FEL amplifier η_{FEL} to be $\eta_{ACC} = 0.4$, $\eta_{SEP} = 0.9$ and $\eta_{FEL} = 0.3$, respectively, we obtain that the total efficiency of the ICF energy driver is equal to $\eta_{TOT} = 0.11$.

Let us estimate output characteristic of the ICF reactor assuming that it is designed by a standard way, i.e. the power of thermonuclear explosion is absorbed by the walls of the reactor chamber, converted into the heat power and then converted into the electrical power.

To estimate output power of the ICF reactor, one should choose the value of the pellet gain Q. In accordance with results of numerical simulations this parameter may reach the values 200 – 1000 (see, for instance, refs. [3], [10]). Assuming that the ICF energy driver initiates thermonuclear explosion with the energy excess by a factor of 1000, repetition rate to be equal to 40 cycles per second, the efficiency of thermonuclear power conversion into the electrical power to be equal to 0.4, the ICF reactor heat and electrical power are equal to 40 GW and 16 GW, respectively. The ICF energy driver itself consumes about of 400 MW of electrical power.

5 FEL amplifier

The FEL amplifier for the ICF reactor consists of 64 parallel channels and each channel is a multi-stage FEL amplifier with 90 stages of amplification. Each FEL amplifier channel provides amplification of a single optical bunch using the scheme of the optical power summation (see section 2). Output power of the multi-stage FEL amplifier significantly exceeds the power of a single electron bunch (in the presented numerical example – by a factor of 30). Such an FEL amplifier meets all the requirements to be the ICF energy driver. Using the electron driving beam with the energy $\mathcal{E} = 3$ GeV, peak current $I_{peak} =$ 2 kA, number of bunches in a train $N = 6440$, it provides 1 MJ energy in optical flash with the radiation wavelength 0.5 μm.

In this section we analyze in details the operation of the multi-stage FEL amplifier. The first stage of the FEL amplifier is destined to amplify relatively weak signal from the master laser ($W_{ext} \simeq$ 1MW) by a factor of the order of 10^5. It is designed by a standard way, i.e. its undulator has a long untapered section and a section with tapered parameters. Output radiation power at the exit of the first stage is of the order of the electron beam power. Subsequent stages of the FEL amplifier amplify a powerful optical beam and provide small amplification per one stage. They operate in a tapered regime from the very beginning and are designed using a scheme of multicomponent undulator (i.e., prebuncher – dispersion section – tapered undulator). It should be noticed that the effect of "optical guiding" [6] does not provide effective focusing of the radiation in these stages. To avoid the radiation power losses, the diaphragm focusing line is used in these stage of the FEL amplifier (see Appendix A for more details).

5.1 First stage of the FEL amplifier

In this section we present the results of calculation of the first stage of the FEL amplifier (see Table 3). It is destined to amplify relatively weak power signal from the master laser ($W_{ext} \simeq$ 1MW). The first stage of the FEL amplifier is designed by a standard way, i.e. its undulator has a long untapered section and a section with tapered parameters. Output radiation power at the exit of the first stage is of the order of the electron beam power. Analysis of the first stage allows one to obtain requirements on the driving electron beam parameters.

Peculiar feature of the first stage is that there is no need in external focusing of radiation, the radiation is concentrated near the electron beam due to the, so called, effect of "optical guiding". So, to calculate characteristics of the FEL amplifier, we use FS2R code (see refs. [11], [12]) developed for calculation of the FEL amplifier with an axisymmetric electron beam.

Table 3: First stage of the FEL amplifier

Undulator	
Undulator period λ_w, cm	15
Undulator field H_w, kG (entr./exit)	10.8 / 9.6
Length of untapered section, m	17.7
Total undulator length, m	64.2
Radiation	
Radiation wavelength λ, μm	0.5
Input power W, MW	1
Output power W, GW	480
Efficiency η, %	8
Reduced parameters	
Diffraction parameter B	0.31
Energy spread parameter $\hat{\Lambda}_T^2$	0.025
Space charge parameter $\hat{\Lambda}_p^2$	0.06
Gain parameter Γ, cm^{-1}	3.7×10^{-3}
Saturation parameter $\beta = \lambda_w \Gamma / 4\pi$	0.0045

Linear mode of the FEL amplifier operation

FEL amplifier can amplify radiation with the wavelength λ satisfying the FEL resonance condition:

$$\lambda \simeq \lambda_w / 2\gamma_z^2 = \lambda_w (1 + Q^2)/2\gamma^2, \qquad (6)$$

where H_w and λ_w are undulator magnetic field and period, respectively, $Q = eH_w\lambda_w/2\pi mc^2$ is the undulator parameter (here and below all the formulae are written for the case of the helical undulator).

In the linear mode of operation, the radiation of the FEL amplifier may be represented as a set of modes. Each mode is characterized with the eigenvalue Λ and the eigenfunction of the transverse distribution of the field $F(\vec{r})$. During the process of amplification, the transverse field distribution remains intact, while its amplitude is growing with the undulator length exponentially, i.e

$$\mid \vec{E}(z, \vec{r}) \mid = \text{const} \times exp(\text{Re}(\Lambda) z) \mid F(\vec{r}) \mid .$$

In the case of axisymmetric electron beam with radius r_0, the eigenvalue equation for

TEM_{mn} mode is of the form [11]:

$$\mu J_{n+1}(\mu)K_n(g) = gJ_n(\mu)K_{n+1}(g), \qquad (7)$$

where n is azimuthal index of the mode, $g = -2iB\hat{\Lambda}$, $\mu = -2i\hat{D}/(1-i\hat{\Lambda}_p^2\hat{D}) - g^2$, $\hat{\Lambda} = \Lambda/\Gamma$ is the reduced eigenvalue,

$$B = \Gamma r_0^2\omega/c$$

is the diffraction parameter,

$$\hat{\Lambda}_p^2 = \Lambda_p^2/\Gamma^2 = 4c^2/(\omega^2 r_0^2\theta_w^2)$$

is the space charge parameter, $\theta_w = Q/\gamma$ is the rotation angle of electron in the undulator,

$$\Gamma = [I\omega^2\theta_w^2/(I_A\gamma_z^2\gamma c^2)]^{1/2}$$

is the gain parameter, I is the beam current and $I_A = m_e c^3/e$. In the case of the Gaussian energy spread, function $\hat{D}$ is given by

$$\hat{D} = i\int_0^\infty \xi \exp[-\hat{\Lambda}_T^2\xi^2 - (\Lambda + i\hat{C})\xi]d\xi,$$

where

$$\hat{C} = C/\Gamma = (2\pi/\lambda_w - \omega/2\gamma_z^2 c)/\Gamma$$

is the reduced detuning from the resonance of the particle with the nominal energy $\mathcal{E}_0$,

$$\hat{\Lambda}_T^2 = \sigma_E^2\omega^2/(2c^2\gamma_z^4\mathcal{E}_0^2\Gamma^2)$$

is the energy spread parameter and

$$\sigma_E = [<(\Delta\mathcal{E}/\mathcal{E})^2> + \gamma_z^4 <(\Delta\theta)^2>^2/4]^{1/2}$$

is the effective width of the energy distribution. We assume the electron beam to be matched with the magnetic system of the undulator which results in the following equilibrium radius r_0 and angle spread $(<(\Delta\theta)^2>)^{1/2}$ of the electron beam:

$$r_0 = (\beta_w\epsilon_n/\gamma\pi)^{1/2}, \qquad (<(\Delta\theta)^2>)^{1/2} = (\epsilon_n/\pi\beta_w\gamma)^{1/2}$$

where $\beta_w = \lambda_w/\sqrt{2}\pi\theta_w$ is the beta-function of the electron beam in the undulator.

Detailed analysis of the FEL amplifier operation has shown that the choice of the FEL amplifier parameters, providing the amplification of the ground TEM_{00} mode, is the most appropriate with respect to attaining of maximal increments and reducing sensitivity to the energy spread [11]. Moreover, the transverse field distribution of this mode is optimal

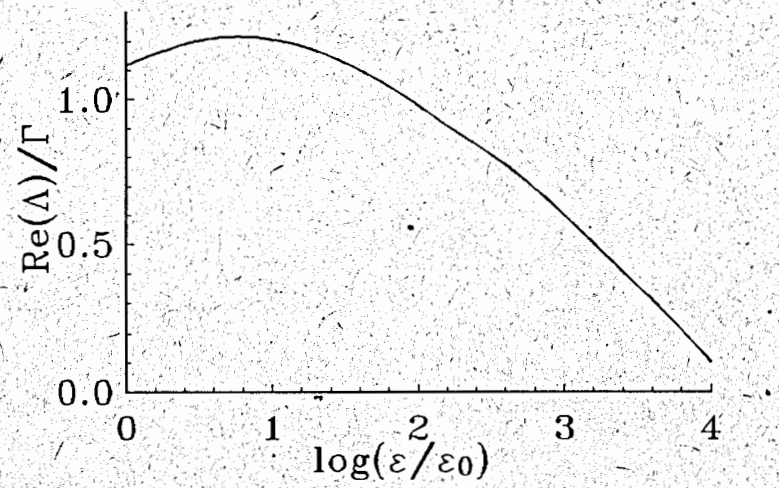

Figure 5: Dependency of the FEL amplifier increment on emittance ($\epsilon_0 = 10^{-8}$cm×rad)

for subsequent matching of the radiation with the diaphragm line. So, we consider below the FEL amplifier tuned to amplify the ground TEM_{00} mode.

Analysis of the linear mode of the FEL amplifier operation enables one to impose restrictions on the values of energy spread and emittance of the driving electron beam. Fig.5 presents the dependence of the reduced increment versus the beam emittance. It is seen from this plot that there is a region of optimal values of emittance when increment achieves its maximal value. At larger emittance there is drastical drop of the increment due to the large spread of the longitudinal velocities of the beam electrons. At small emittance values, a decrease of increment is connected with the growth of the space charge fields, so as transverse size of the matched electron beam is decreased while the beam emittance is decreased. The behaviour of increment in the intermediate region is defined with diffraction effects due to the change of the transverse size of matched electron beam. One can find from Table 2 that for the numerical examples we have chosen the values of the emittance which are slightly larger than those optimal given by the plot in Fig.5. The real reason of such a choice is based on the results of the overall optimization of the undulator length. Indeed, when one uses the electron beam with the emittance providing maximal increment in the linear mode of operation, this make it possible to reduce the length of this part of the amplifier. Then, at the nonlinear stage of the FEL amplifier operation, one should trap a significant fraction of electrons in the regime of coherent deceleration to obtain a high efficiency. Numerical simulations have shown that in this case the action of the space charge field forces to provide a more slow undulator

tapering, which results in a more larger undulator length. An experience obtained on the base of numerical simulations has shown that one should choose such a value of the emittance which results in the value of the space charge parameter $\hat{\Lambda}_p^2 \lesssim 0.1$.

Another important factor influencing significantly on the FEL amplifier operation is the energy spread of the electrons in the beam. The plot in Fig.6 presents the dependence of the increment on the energy spread.

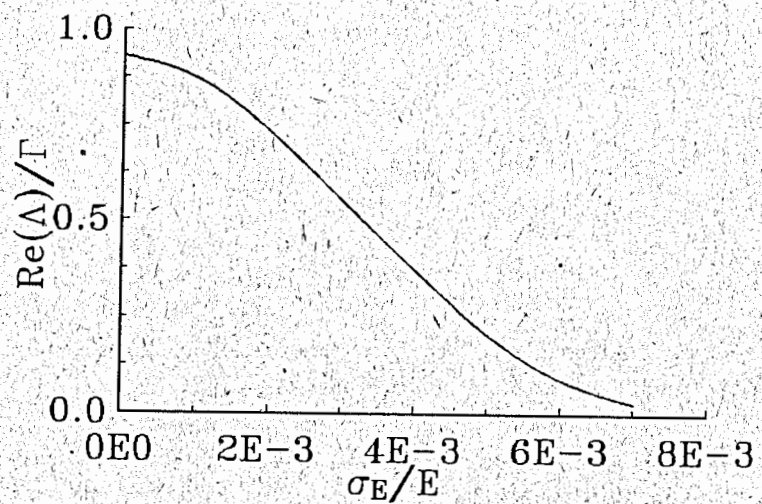

Figure 6: Dependency of the FEL amplifier increment on energy spread

It is seen that increment visibly drops at $\Delta\mathcal{E}/\mathcal{E} \gtrsim 0.2\%$. Numerical simulation of the nonlinear mode of the FEL amplifier operation have shown that the final FEL efficiency drastically drops when the energy spread exceeds this value.

Using this analysis, we have chosen the emittance and the energy spread of the driving electron beam to be equal to $\epsilon = 1.6 \times 10^{-6}$ cm·rad ($\epsilon_n = 3 \times 10^{-3}$ cm·rad) and $\sigma/\mathcal{E}_0 = 0.1$ %, respectively.

FEL amplifier noise

In the case under consideration the FEL amplifier noise is defined mainly by random fluctuations of the electron beam density and effective power of the noise signal at the FEL amplifier entrance is given with the expression [13]:

$$W_{sh} \simeq eI\omega\gamma_z^2\theta_w^2/c \qquad (8)$$

For the FEL amplifier parameters presented in Table 3, the effective power of shot noise at the FEL amplifier entrance is equal to $W_{sh} \simeq 40$ W, so the chosen value of the master oscillator power $W_{ext} = 1$ MW is much more than this value.

Optimization of the undulator length and the FEL amplifier output characteristics

During the process of the radiation amplification the electrons lose their energy which leads to desynchronism of the electrons an the electromagnetic wave. In the case of the undulator with the fixed parameters these results in a situation when at some undulator length the most fraction of electrons shifts to an accelerating phase of the ponderomotive well and the electron beam begins to take off the energy from the electromagnetic wave. The radiation power at the saturation is of an order of [12]:

$$W_{sat} \simeq \beta\mathcal{E}_0 I/e, \qquad (9)$$

where

$$\beta = \lambda_w\Gamma/4\pi. \qquad (10)$$

Usually the gain length $l_g = 1/\Gamma$ is much more than the undulator period which results in a low saturation efficiency

For the FEL amplifier parameters presented in Table 3, the saturation efficiency is $\eta_{sat} \sim 0.5$ %. The method of the FEL amplifier efficiency increase by the undulator parameters tapering is a widely known one [4], [14], [15]. There is a lot of possibilities of undulator tapering and here we have chosen for numerical example only one of them, namely the undulator field decrease at fixed undulator period λ_w. We have performed a set of calculations to obtain optimal conditions of the tapering. As a result, a linear law of tapering has been chosen. Undulator tapering begins at the undulator length equal to 17.7 m and the required level of the radiation power is achieved at the undulator length $L \sim 64$ m. At the undulator exit, the change in the undulator magnetic field is $\Delta H_w/H_w = 10$ %. A phase analysis shows that about 75 % of the electrons trap in the regime of coherent deceleration.

Fig.7 presents the dependency of the FEL amplifier output power on the reduced detuning $\hat{C} = C/\Gamma = (2\pi/\lambda_w - \omega/2\gamma_z^2 c)/\Gamma$. This plot enables one to find restrictions on the values of systematical drifts: frequency of the master oscillator $\Delta\omega/\omega = 2\beta \cdot \Delta\hat{C}$; energy deviation $\Delta\mathcal{E}/\mathcal{E} = \beta \cdot \Delta\hat{C}$; undulator field $\Delta H_w/H_w = \beta(1+Q^2) \cdot \Delta\hat{C}/Q^2$ (here the reduced bandwidth of the amplifier $\Delta\hat{C}$ is determined by the requirements on the stability of the output power level). It is seen from the plot in Fig.7 that systematical drifts ~ 1 % of the above mentioned parameters do not influence significantly on the FEL amplifier output power.

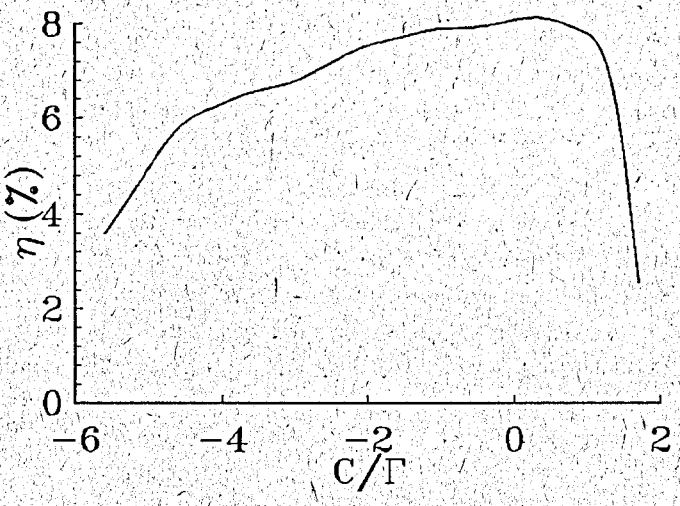

Figure 7: Output FEL amplifier power versus detuning

It should be noticed here that the notion of energy spread needs some explanation. We have obtained above that the FEL amplifier operates successfully when the energy spread in the beam is rather small, $\delta\mathcal{E}/\mathcal{E}_0 \simeq 0.1$ %. Physical sense of this energy spread is that it is instantaneous, i.e. particles of the beam with the mean energy $\mathcal{E}_i$ occupy finite region in the phase space. On the other hand, the driving electron beam, produced by the RF accelerator, has finite phase extent with respect to the accelerating RF wavelength. It results in a drift of the mean energy of the particles along the beam. Using Table 2, one can obtain that the half-width of this distribution is equal to $\delta\mathcal{E}/\mathcal{E}_0 \simeq (1/4)(\pi l_b/\lambda_{rf})^2 \simeq 0.5$ %. To be strict, this energy drift does not increase the phase space occupyed by the beam and in the case under consideration it does not influence significantly on the FEL amplifier operation due to local interaction of the radiation with the electrons in the beam. Indeed, characteristic scale of the interaction region is defined by the slippage length of the optical beam with respect to electron beam, which is about of a fraction of millimeter. So, at each point the radiation interacts with the electrons having approximately instantaneous energy spread equal to $\delta\mathcal{E}/\mathcal{E}_0 \simeq 0.1$ %. The drift of the mean energy along the beam equal to 0.5 %, in accordance with the plot presented in Fig.7, does not influence on the FEL output power, because all parts of the electron beam interact resonantly with the optical beam.

5.2 High efficiency FEL stages

We have considered above the operation of the first stage of the multi-stage FEL amplifier. This stage provides amplification of relatively small signal of the master oscillator ($W_{in} \simeq 1$ MW) up to the power comparable with the power of the electron beam. While this scheme is optimal for amplification of a small signal, it is completely nonoptimal when the input optical power is comparable with the electron beam power. So, we propose to use in the subsequent stages the FEL amplifier with the multicomponent undulator which consists of a prebuncher, dispersion section and tapered undulator. Such an FEL amplifier configuration allows one to provide effective capture of electrons into the regime of coherent deceleration and attain a high efficiency.

In the presented paper we propose to use a periodic diaphragm line for focusing the radiation. It has a form of a sequence of screens with holes. When Fresnel number is large, eigenmodes of such a line have rather small diffraction losses. For instance, in a visible wavelength range, at the radius of the hole about of 1 cm and the distance between the screens about of 1 m, diffraction losses of the ground eigenmode are about of 0.01 % per one diaphragm.

Operation of the multistage FEL amplifier proceeds as follows. In the initial stages a transitional processes take place: the optical power amplification and formation of the optical field eigenmode. After passing a large number of stages, the amplification coefficient G becomes to be small and the transverse field distribution is settled corresponding to the ground TEM_{00} mode of the diaphragm focusing line. Estimations have shown that this process is lasted approximately 10 amplifier stages. As a result, calculation of the stages from 10 to 90 can be performed using one-dimensional theory in approximation of the given optical field amplitude.

A choice of the multi-stage amplifier parameters

General approach to the analysis of the high-efficiency FEL amplifier stages is presented in Appendix B. Here we present the results of numerical simulations.

Using the requirements on the output characteristics of the ICF energy driver, we have fixed in the previous sections such parameters as the energy and current of the electron beam, number of the FEL amplifier stages and their efficiency. These parameters are as follows: $\mathcal{E}_0 = 3$ GeV, $I = 2$ kA, $N_s = 90$, $\eta_{FEL} = 0.3$. Values of the emittance and the energy spread of the driving electron beam are defined by the requirements of efficient operation of the first stage and are equal to $\epsilon \simeq 1.6 \times 10^{-6}$ cm·rad and $\sigma/\mathcal{E}_0 \simeq 10^{-3}$.

Assuming the undulator period to be $\lambda_w = 20$ cm nd radiation wavelength to be

$\lambda = 0.5$ μm, we obtain:

$$Q_w(0) \simeq 13, \qquad \theta_w \simeq 2.2 \times 10^{-3}, \qquad \gamma_{z0}^{-2} \simeq 4.9 \times 10^{-6}.$$

The gain parameter is given with the formula (B.5):

$$\tau = 2.3 \times 10^{-4} l_w^3 / R^2, \tag{11}$$

Here and below l_w is in meters and the diaphragm radius R is in cm. Factor g is given with the formula (B.7):

$$g \simeq 1.6 \times 10^{-2} / l_w, \tag{12}$$

Assuming the energy spread in the beam to be gaussian with $\sigma/\mathcal{E}_0 \simeq 10^{-3}$, the energy spread parameter $\hat{\Lambda}_T$ from expression (B.14) is given with:

$$\hat{\Lambda}_T = \sigma / \mathcal{E}_0 g \simeq 6.3 \times 10^{-2} l_w, \tag{13}$$

At a large number of the stage (i.e. at $n > n_0 = 10$), the transition processes are finished and the field amplification may be calculated in the framework of one-dimensional model using a small-gain approximation (see Appendix B). In the presence of focusing diaphragm line two competing processes take place: one of the field amplification given with the gain factor G and another – of the field damping given with the damping factor K. Total FEL efficiency η_{FEL} is connected with the electron efficiency η by the relation:

$$\eta_{FEL} = (1 - K/G)\eta.$$

Here damping factor K can be calculated using formulae of Appendix A and the gain factor G – by formulae of Appendix B. Estimations have shown that the number of transitional stages is approximately equal to $n_0 \simeq 10$ and their average efficiency is approximately equal to a half of the efficiency of the high-efficiency stage. So, we may write the following formulae for the output power of the multi-stage FEL amplifier with the number of stages equal to n ($n > n_0$):

$$W_n \simeq [0.5 n_0 + (n - n_0 - 1)] \eta_{FEL} W_b = n' \eta_{FEL} W_b, \tag{14}$$

where W_b is the power of electron beam, $n' = n - 0.5 \times n_0 - 1$. So as the number of transitional stages is equal to $n_0 = 10$, then $n' = n - 6$. Field amplification factor in the n-th stage is given with the formula:

$$G_n \simeq \eta W_b / 2n' \eta_{FEL} W_b = \eta / 2n' \eta_{FEL}. \tag{15}$$

Taking into account that the field distribution of the ground mode TEM_{00} of the diaphragm line is $|\tilde{E}| \propto J_0(\mu_{01} r/R)$ (see Appendix A), we may calculate reduced amplitude of radiation field after n-th stage:

$$\hat{u}_n = 0.24 \times [n' \eta_{FEL}]^{1/2} l_w^2 / R. \tag{16}$$

Damping factor K may be calculated using formula (A.5). Assuming the period of diaphragm line to be $L = 0.5$ m, we obtain:

$$K \simeq 3.7 \times 10^{-5} l_w / R^3. \tag{17}$$

The next step of our study is the optimal choice of the values of the undulator lengths l_w and diaphragm radiuses R as functions of the stage number n. We assume that diaphragm radiuses R is changed adiabatically along the diaphragm line. We confine optimization process by two conditions. First, we assume the efficiencies to be equal for all stages. Second, the raté of radiation damping to amplification K/G is assumed to be constant. The latter condition means that the heat load on the diaphragm line is almost uniform in all the stages. As a result, we obtain:

$$K/G \propto \frac{n' l_w(n')}{R^3(n')} = \text{const}. \tag{18}$$

Using formulae (B.9), (11) and (16) we obtain once more relation between the values of l_w and R:

$$\eta \propto g\hat{u} \propto \frac{(n')^{1/2} l_w(n')}{R(n')} = \text{const}. \tag{19}$$

Using relations (18) and (19), we obtain:

$$l_w \propto (n')^{-1/4}, \qquad R \propto (n')^{1/4}. \tag{20}$$

Then, using formulae (11) – (13) and (16), we obtain the following parametric dependencies:

$$g \propto (n')^{1/4}, \quad \tau \propto (n')^{-5/4}, \quad \hat{\Lambda}_T \propto (n')^{-1/4}, \quad \hat{u} \propto (n')^{-1/4}, \quad \hat{\alpha} \propto (n')^{-1/4}. \tag{21}$$

It is useful to notice that the depth of the undulator field tapering

$$|\Delta \hat{H}_w| / H_w(0) = \hat{\alpha} g$$

does not depend on the number of the stage. Analysis of the obtained parametric relations together with relation (B.16) shows, that the similarity of the stages is not universal due to the dependence of the value of $\hat{\Lambda}_T/(\hat{u})^{1/2}$ on the number of stage:

$$\hat{\Lambda}_T / (\hat{u})^{1/2} \propto (n')^{-1/8}.$$

Nevertheless, this dependence is rather weak and does not influence significantly on the FEL efficiency.

The corresponding parametric dependencies for the prebuncher and drift space are defined with the relations:

$$(\delta\hat{P})_p = \hat{u}\hat{l}_p \propto \hat{u}^{1/2}, \qquad (\delta\hat{P})_p\hat{l}_d = \text{const.},$$

which results in

$$\hat{l}_p \propto (n')^{1/8}, \qquad \hat{l}_d \propto (n')^{1/8}. \tag{22}$$

Phase shift $\delta\psi$ in the drift space is equal for all stages, so it is sufficient to find it for one of the stages. For definiteness, we consider the last, 90-th stage. We perform optimization aiming a goal to attain minimal length of the stage at fixed FEl efficiency $\eta_{FEL} = 0.3$. Numerical simulations have shown that the choice of

$$l_w = 40 \text{ m}, \qquad R = 1 \text{ cm}.$$

is close to the optimal values. According to relations (11) – (13) and (16), such a choice corresponds to the following reduced parameters (see Appendix B):

$$g = 4 \times 10^{-4}, \qquad \tau = 14.7, \qquad \hat{\Lambda}_T = 2.5, \qquad \hat{u} = 2 \times 10^3.$$

Parameter of the tapering depth is chosen to be $\hat{\alpha} = 1.5 \times 10^3$ which results in the decrease of the magnetic field along the main undulator:

$$|\Delta H_w| / H_w(0) = \hat{\alpha} g = 0.6.$$

Parameters of prebuncher and drift space are as follows:

$$\hat{l}_p = 6.3 \times 10^{-3}, \qquad \hat{l}_d = 0.11, \qquad \delta\psi = 1.$$

When calculating the length of prebuncher, one may obtain that its length may be not multiple or less than undulator period. In this case parameters of prebuncher (period and magnetic field) should be chosen to provide calculated beam bunching for a corresponding stage. The number of prebuncher periods is usually about of 3 – 4 and their total length is much less than the length of the main undulator. As for the length of the drift space $l_d = \hat{l}_d l_w(1 + Q + 0^2)$, in some cases it may be rather large. In this case the drift space should be replaced with equivalent dispersion section which length is much less than the length of the main undulator.

The extraction efficiency of the 90-th stage is equal to $\eta \simeq 0.4$. Figs. 8a, 8b and 8c illustrate phase distribution of the particles at the entrance, in the middle and at the exit of the main undulator, respectively. Using formulae (15) and (17), we obtain the values of the field amplification and field losses in the 90-th stage:

$$G \simeq 7.5 \times 10^{-3}, \qquad K = 1.5 \times 10^{-3}, \qquad K/G \simeq 0.2,$$

(a)

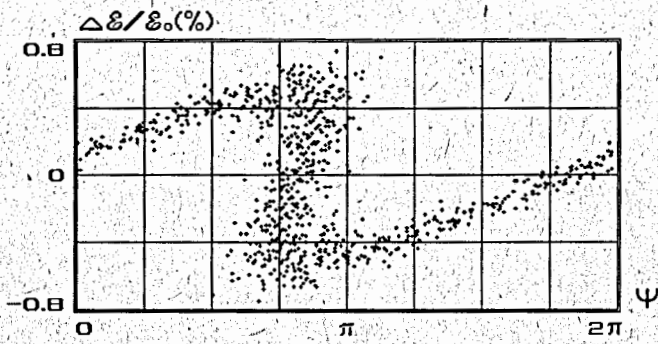

(b)

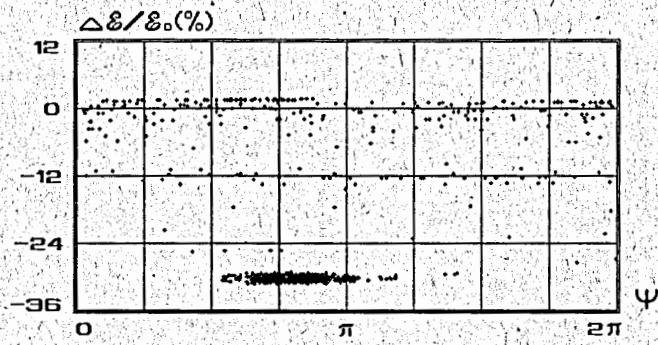

(c)

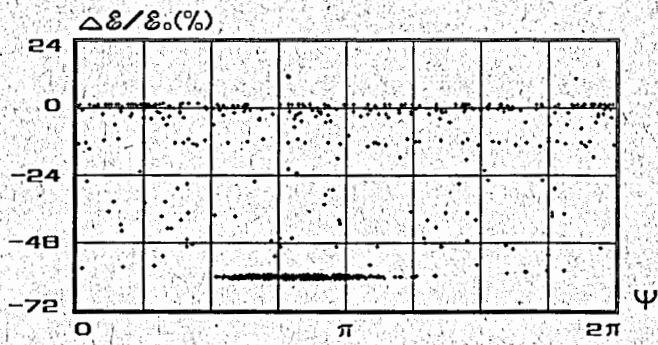

Figure 8: Phase distribution of the particles in the 90-th FEL amplifer stage: (a) – entrance, (b) – middle and (c) – exit of the main undulator

6.2 Separation system

There are six stage in the separation system providing separation of the electron bunch train by sequential scheme. Pulse duration of the kicker magnets are equal to 12.8 μs, 6.4 μs, 3.2 μs, 1.6 μs, 0.8 μs and 0.4 μs for the 1st, 2nd, 3rd, 4th, 5th and 6th stages, respectively. To provide a high efficiency of separation system, e.g. $\eta_{SEP} \simeq 0.9$, kicker magnets should provide rise (fall) time about of 50 ns. Such kicker magnets may be manufactured at the present level of acceleration technique R&D, kicker magnets of the SLC damping ring provide parameters close to those required [18].

6.3 Undulator

Undulators of the FEL amplifier should have period $\lambda_w \simeq 15 - 20$ cm and magnetic field $H_w \simeq 7 - 10$ kGs. It should have rather large aperture to place diaphram focusing line inside. Taking into account these requirements, it seems to be natural to construct a superconducting undulator. It should be noted that the first FEL lasing was obtained with the superconducting undulator [19, 20]. That undulator had the period $\lambda_w = 3.2$ cm and total length 5 m. Amplitude of the magnetic field $H_w = 10$ kG was attained at the current density in superconducting windings $j_s = 700$ A/mm^2. Bifilar windings were mounted on the tube with diameter 1 cm. To scale these parameters to the case under consideration, we use the following expression for the magnetic field at the undulator axis [21]:

$$H_w = \frac{I_w}{\pi R_w}[\zeta^2 K_0(\zeta) + \zeta K_1(\zeta)], \qquad (24)$$

where $\zeta = \kappa_w R_w$, $\kappa_w = 2\pi/\lambda_w$, I_w is the current in the winding, R_w is the winding radius and K_0 and K_1 are the modified Bessel functions (here it is assumed that the transverse dimensions of the winding Δ and δ are much less than the winding radius R_w). The extrapolation of the results of ref. [20] to the case under study may be performed by the increase of the winding current I_w and all geometrical dimensions, namely R_w, λ_w, Δ and δ by $6 \div 7$ times. So as the winding current is equal to $I_s = j_s \delta \Delta$, one can see that the requirement on the value of the critical current is diminished significantly and there is a reserve to increase the winding current. Thus, the undulator of the first free-electron laser may be considered as a scaled model of the undulator for the FEL based ICF energy driver.

6.4 Cryogenic system

Cryogenic system should provide cooling of magnetic system of the FEL amplifier. It may be designed to be rather effective, using, for instance, a package placement of the

FEL amplifier elements. In this case the cryogenic system will consist of 1432 cryostats of two types. One type of cryostats provides cooling of a package of 8 undulators and another – of 8 magnetic snakes. It seems to be perspective to use a multi-refrigerators system integrated into the cryostat which provides effective cooling without the use of external coolant. It consists of a 4° K closed-cycle He gas refrigerator and a 20/80° K two-stage closed-cycle He gas refrigerator adopted to cool 40° K and 80° K heat shields and other components of the cryostat [22].

In the case under consideration, the summed static heat load to 80° K shield, 40° K shield and to the liquid He vessel will be about of 300 W, 100 W and 10 W per one cryostat, respectively. Assuming the electrical power consumption per 1 W coolant capacity to be 20 W, 100 W and 700 W for 80° K, 40° K and 4° K refrigerators, respectively, total electrical power consumption will be about of 25 kW per one cryostat. As a result, the cryogenic system of the FEL magnetic system will consume about of 35 MW of electrical power which constitute relatively small fraction of the total power consumption (400 MW).

7 Discussion

When preparing the conceptual project of the FEL based ICF reactor, we have based at the present level of accelerator technique R&D. When considering future perspectives of the proposed approach, it should be noticed that the parameters of the commercial FEL based ICF reactor (see Table 1) are not ultimate. The main reserve to increase its power and efficiency is to increase the power and efficiency of the driving accelerator. In the presented study we have based on the klystron efficiency $\eta(\text{klystron}) = 0.5$, a level which is well mastered by industry for pulsed klystrons of decimeter wavelength range. It seems to be rather realistic that the efficiency of pulsed klystrons may be increased up to the value about of $\eta(\text{klystron}) \simeq 0.7 - 0.8$ in the nearest future. Such a value of the klystron efficiency has been achieved at CW klystrons developed for RF systems of circular colliders. For instance, TH 2089 klystron, operating at 350 MHz frequency, provides output RF power 1 MW at 70 % efficiency. The use of klystrons with such an efficiency will allow one to increase the ICF energy driver efficiency from 11 % up to 16 %. Another reserve to increase the ICF reactor power is the increase of repetition rate. In the proposed project, repetition rate is limited by the average power of klystrons. The use of klystrons with the average output RF power 100 kW will enable to increase the repetition rate up to 120 cycles per second and to increase electrical power of the reactor from 16 GW up to 50 GW.

The thorough analysis presented in this paper have shown that the FEL technique enables one to construct the energy driver which fits the requirements to be the energy

driver for inertial confinement fusion. We have shown above that such a system may be realized at the present level of accelerator technique R&D. Nevertheless, it should be emphasized that despite many pieces of the proposed equipment have been developed for other applications, there are no operating FEL amplifiers with the parameters close to those required. So, the basic idea of the proposal, namely a possibility to construct multi-stage FEL amplifier, requires experimental verification. To perform such a verification, there is no need to build a full-scale facility. It may be done, for instance, by constructing a model of the FEL amplifier with the number of amplification stages about of 10. Such a test facility requires electron accelerator providing acceleration of 10 electron bunches (bunch spacing about of 4 ns, $\mathcal{E} \simeq 3$ Gev, peak current $I \simeq 2$ kA, emittance $\epsilon_n \simeq 3 \times 10^{-3}$ cm·rad, energy spread $\sigma_E/\mathcal{E}_0 \simeq 10^{-3}$). Micropulse duration of this accelerator may be done rather short, about of 10 ps, in this case slippage effect is almost negligible. The energy stored in 10 bunches will be about of 600 J, so such a test accelerator may operate in L-band RF wavelength range in a regime of stored RF energy. At accelerating gradient about of 30 MV/m, its length will be about of 100 m. An accelerator facility with parameters close to those required is developed, for instance, in the framework of superconducting linear collider project TESLA [23].

Experiments, carried out at a such relatively low-cost facility will reveal a possibility to construct in the nearest future a full-scale FEL based energy driver for inertial confinement fusion.

Appendix A. Diaphragm focusing line

As a rule, lens systems are used for transporting and focusing of optical radiation. While this technique is appropriate at a relatively small radiation power, it is completely unfit for focusing and transporting of powerful laser beams with the average and peak radiation power about of one megawatt and several hundreds terawatts, respectively. Nevertheless, this problem may be solved by using diaphragm focusing line which has a form of periodically spaced screens with round holes.

Basic consideration

Diaphragm focusing line operates as follows. Consider electromagnetic wave passing along the sequence of diaphragm. When electromagnetic wave diffracts at the first diaphragm, it produces diffraction pattern in the plane of the next diaphragm. When the second diaphragm is placed in the main maximum of the diffraction pattern, diffraction losses are minimal. Further, sideband maxima of the diffraction pattern produced by the second diaphragm are less than that of the first pattern, etc. When the wave passes a large

number of diaphragms, the field eigenmode is formed which has low diffraction losses. For the first time eigenmodes of the diaphragm line have been calculated numerically by Fox and Li [24] and later have been obtained analytically by Veinstein [8].

To get a deeper insight into the role of diffraction effects for forming the eigenmode in the diaphragm line, we, following by ref. [25], study the problem of the diffraction of the plane wave at periodical sequence of completely absorbing semi-infinite screens (see Fig.9).

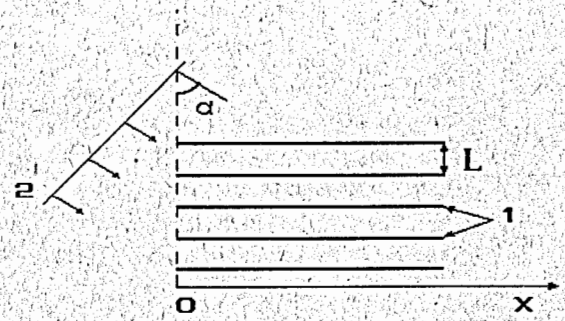

Figure 9: Diffraction of plane wave at semi-infinite screens. Here: 1 – screens, 2 – incident wave.

Period of the structure is equal to L and direction of the wave propagation forms a small angle α with the plane perpendicular to the edges of the screens. We assume that

$$\alpha^2 \ll \lambda/(\pi L),$$

where λ is the wavelength.

The field of the wave, diffracted at the edge of totally absorbing screen, can be presented as a sum of two waves: the wave which does not exist in the region of geometrical shadow and is unperturbed outside it, and cylindrical wave which is produced by a image source located at the edge of the screen [26]. In the considered geometry, the field $u_1(x)$ of the wave, diffracted at the first screen is given with the expressions:

$$u_1(x) = \begin{cases} u_0 - (u_0/\pi^{1/2})F(\xi), & x < 0 \\ (u_0/\pi^{1/2})F(\xi), & x > 0 \end{cases} \qquad \text{(A.1)}$$

where u_0 is the amplitude of incident plane wave,

$$F(\xi) = \int_{\xi}^{\infty} \exp(i\tau^2) d\tau$$

is Fresnel integral and $\xi = (\pi/\lambda L)^{1/2}x$. Substituting approximate expression for Fresnel integral

$$F(\xi) = i\exp(i\xi^2)\left[2\left[\xi + \sqrt{i/\pi}\right]\right]^{-1}$$

into formula (A.1) for $u_1(x)$ we obtain the field distribution in the region of geometrical shadow:

$$u_1(x) \simeq A(x)\exp(ikx^2/2L),$$

where $k = 2\pi/\lambda$ and $A(x)$ is slowly changing function.

When unperturbed wave is diffracted at the second edge, it produces another cylindrical wave with the image source located at the edge of the second screen. Besides this wave, there exists also unperturbed plane wave which produces another cylindrical wave at the third screen, etc. As a result, the field of diffracted wave is presented in the region $x < 0$ by a superposition of cylindrical waves produced by image sources located at the edges of all the screens and with amplitudes decreasing with the deflection of their propagation off the direction of propagation of the initial wave.

Due to the interference of a large number of cylindrical waves, there exists a series of discrete directions where amplitudes of these waves are summed. It is illustrated with Fig.10.

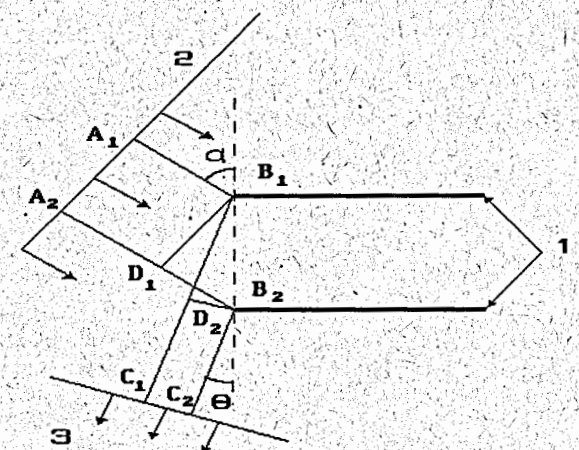

Figure 10: Diffraction of plane wave at semi-infinite screens. Here: 1 – screens; 2 – incident wave; 3 – diffracted wave.

The difference of paths $A_1B_1C_1$ and $A_2B_2C_2$ is equal to the difference of paths D_1B_1 and B_2D_2, which means that the waves produced by edges of the adjacent screens are summed

when

$$kL(\theta^2 - \alpha^2)/2 \simeq 2\pi n,$$

where n is integer number. At the intermediate directions, the field amplitude takes zero value due to interference effects. At $\alpha^2 \ll \lambda/(\pi L)$ the amplitude of the "reflected" wave with $n = 0$ and $\theta_0 = \alpha$ significantly exceeds the amplitudes of another waves.

So, when the incident angle of the wave is rather small, ($\alpha^2 \ll \lambda/(\pi L)$), the radiation does not absorb and is dispersed due to diffraction effects and the most fraction of the power is in the "reflected" wave.

Using analytical techniques, Veinstein has obtained coefficient of diffraction reflection R_0 of the plane wave from the sequence of semi-infinite periodical screens [8]:

$$R_0 = -\exp\left[-\beta_0(1-i)s\right], \qquad (A.2)$$

where $s = \alpha(kL)^{1/2}$ and $\beta_0 = 0.824$. When factor s is decreased, the absolute value of R_0 is approached to the unity. The phase multiplier in the right-hand part of eq. (A.2) corresponds to the phase shift not equal to π. As a result, the process of reflection takes place as if a mirror should be placed slightly farther then the plane of the screen edges.

Let us derive one important consequence of eq. (A.2). Resulting field of incident and reflected wave may be presented in the form:

$$E(x,z,t) = u(x)\exp(ikz - i\omega t) = [A\exp(ik_x x) + B\exp(-ik_x x)]\exp(ikz - i\omega t),$$

where $k_x/k_z \simeq \alpha$, $k_x^2 + k_z^2 = 4\pi^2/\lambda^2$ and $\omega = 2\pi c/\lambda$. At the plane of the screen edges the ratio of reflected and incident waves B/A is equal to R_0, which results in

$$u(x) = A\left[\exp(ik_x x) + R_0\exp(-ik_x x)\right].$$

One can obtain that the value of logarithmic derivation of $u(x)$ at the plane of the screen edges is equal to:

$$d\ln(u)/dx|_{x=0} = (1/u)du/dx|_{x=0} = ik_x(1-R_0)/(1+R_0).$$

Assuming factor s to be small and replacing $\exp\left[-\beta_0(1-i)s\right]$ by $1-\beta_0(1-i)s$, we obtain

$$(1-R_0)/(1+R_0) \simeq \left[\beta_0(1-i)k_x\sqrt{\lambda L/(8\pi)}\right]^{-1},$$

and

$$d\ln(u)/dx|_{x=0} = -\left[\beta_0(1+i)\sqrt{\lambda L/(8\pi)}\right]^{-1}. \qquad (A.3)$$

Peculiar feature of the latter formula is that the term k_x is completely excluded from it, which allow one to use it as a universal boundary condition. Let us consider, for

instance, a periodical diaphragm line formed by a sequence of slits in absorbing screens. Transverse dimension of the slits is equal to $2a$ and coordinates of the screen edges are equal to $x = \pm a$. Eigenfunctions $u_j(x)$ of such a diaphragm line are the solutions of the homogeneous equation:

$$d^2u_j/dx^2 + k_j^2 u_j = 0$$

and satisfy boundary conditions

$$\left[u_j \pm (1+i)\beta_0\sqrt{\lambda L/(8\pi)}du_j/dx\right]_{x=\pm a} = 0.$$

In the first approximation of a small parameter $M = (8\pi N_F)^{-1/2}$, where $N_F = a^2/(\lambda L)$ is Fresnel number, functions u_j are given with

$$u_j(x) = \begin{cases} \cos[\pi j(1-\Delta)x/(2a)], & j = 1,3,\dots \\ \sin[\pi j(1-\Delta)x/(2a)], & j = 2,4,\dots \end{cases} \qquad (A.4)$$

where $\Delta = (1+i)\beta_0 M$. Validity region of these results is that parameter j must satisfy inequality

$$\pi^2 j^2 M^2 \ll 1.$$

Substituting $k_x = \pi j(1-\Delta)/(2a)$ into relation

$$k_x^2 + k_z^2 = \omega^2/c^2 = 4\pi^2/\lambda^2$$

we obtain expression for k_z:

$$k_z L \simeq \omega L/c - \pi^2 j^2 M^2/2 + \pi^2 j^2 M^3(1+i)\beta_0.$$

For the j-th eigenmode, a fraction of the radiation power losses per passage of one diaphragm is given with the relation:

$$2\mathrm{Im}(k_z L) = 2\pi^2 j^2 \beta_0 M^3.$$

Axisymmetric diaphragm line

On the base of previous study we can calculate parameters of the axisymmetric diaphragm line. We assume the radius of the hole to be rather large, $R \gg \lambda$. Eigenfunctions $\Phi_m(r,\varphi)$ of the axisymmetric diaphragm line have the form:

$$\Phi_m = u_{mj}(r)\exp(-\mathrm{im}\varphi), \qquad m = 0,1,2,\dots$$

Functions u_{mj} are the solutions of the homogeneous equation:

$$r^2 d^2u_{mj}/dr^2 + rdu_{mj}/dr + (k_{mj}^2 - m^2)u_{mj} = 0$$

and satisfy boundary conditions:

$$\left[u_{mj} + (1+i)\beta_0\sqrt{\lambda L/(8\pi)}du_{mj}/dr\right]_{r=R} = 0.$$

In the first order of a small parameter $M = (8\pi N_F)^{-1/2}$, where $N_F = R^2/(\lambda L)$ is Fresnel number, functions u_{mj} have the form [8], [25], [27]:

$$u_{mj} = J_m^*(k_{mj}r),$$

where $k_{mj} = \mu_{mj}(1-\Delta_0)/R$, $\Delta_0 = (1+i)\beta_0 M$, μ_{mj} is j-th root of the Bessel function of the m-th order (i.e. $J_m(\mu_{mj}) = 0$). Substituting expressions for k_{mj} into relation

$$k_z^2 + k_{mj}^2 = \omega^2/c^2$$

we obtain expression for k_z :

$$k_z L \simeq \omega L/c - 2\mu_{mj}^2 M^2 + 4\mu_{mj}^2 M^3(1+i)\beta_0.$$

For the TEM_{mj} eigenmode, a fraction of the radiation power losses per passage of one diaphragm is given with the relation:

$$2\mathrm{Im}(k_z L) = 8\mu_{mj}^2 M^3 \beta_0. \qquad (A.5)$$

Imperfections of diaphragm line

Let us study the influence of imperfections in the diaphragm line on its properties (see, e.g. ref. [25]).

When one of the screens is shifted off the axis, it may cause distortion of the amplitude and phase of the scattered wave. To estimate the change in the amplitude, one should remember that the amplitude of the cylindrical wave, produced by the edge of the screen, is proportional to the Fresnel integral $F(\xi)$ in the region of the next screen and is decreased by a factor of 2.5 at $|\ x\ | > (\lambda L/\pi)^{1/2} = \Delta_1$. So, the region of $x > \Delta_1$ is the region of shadow. If the screen is shifted off the axis by the value $\delta \gtrsim \Delta_1$, either this screen or the next screen falls into the region of the shadow and does not produce diffracted wave.

To estimate phase errors, we consider the drawing presented in Fig.10. One can see that the shift of the screen by the value δx in the transverse direction causes the phase shift of the wave, propagated by the angle θ

$$k\delta x(\sin\alpha + \sin\theta) \simeq k\delta x(\alpha + \theta).$$

For the reflected wave, the change in the phase equal to π is achieved at $\delta x = \Delta_2 = \lambda/(4\alpha)$. At small angle approximation $\alpha^2 \ll \lambda/(\pi L)$, it results in the inequality $\Delta_2 \gg \Delta_1$ which

means that the value of admissible shift of the screen is defined mainly by aperture restrictions but not by phase distortions. So, requirements on the accuracy of transverse adjustment of the screens is given with $\delta x \ll \Delta_1 = (\lambda L/\pi)^{1/2}$.

As for the accuracy of the longitudinal adjustment of the screens, it is defined mainly by the effect of the higher order modes production. A relative power of this effect is given with the ratio of the error in the period δL to the period L. When the screens are adjusted with the accuracy about of $\delta L \simeq 10^{-2}$ cm (which is usual in the accelerator technique), parameter $\delta L/L$ will be of the order of 10^{-4} and irregularity of the diaphragm focusing line does not result in the extra diffraction losses.

In conclusion of this section it should be noticed that there is no need to use completely absorbing screens in the diaphragm line. Moreover, it would be preferable to use reflecting screens. At accepted limitations, reflecting screens are almost identical to absorbing screens with respect to diffraction effects, while the problems of the heat load on the edges of diaphragms are not so severe.

Appendix B. Calculation of a high-efficiency FEL amplifier stage

In the present section we describe briefly the method of calculating the FEL amplifier stage with a high efficiency. When the field is amplified in the multi-stage FEL amplifier, the process of the field eigenmode formation, corresponding to the ground TEM_{00} mode of the axisymmetric diaphragm line takes place (see section 5 and Appendix A). At a large number of the stage, the field amplitude eigenmode is settled and the field gain G per one stage becomes to be small. These reveals a possibility to calculate the process of the field amplification using one-dimensional model in approximation of the small field gain.

So as the optical field power is rather large in this case, it becomes to be optimal to use the FEL amplifier with multicomponent undulator consisting of a prebuncher, dispersion section and main undulator with tapered parameters. It operates as follows. At first, the electron beam is modulated by the energy in the prebuncher. Then it is bunched in the drift space (or dispersion section). Finally, the bunched beam is fed to the entrance of the main undulator with the tapered parameters where a significant fraction of electrons traps into the regime of coherent deceleration.

For simplicity, we begin the analysis of the field amplification in the multicomponent undulator with the case of a small FEL efficiency. This allow one to write down the FEL equation in a more simple form, neglecting the change of the electron energy $\mathcal{E}$ and undulator field H_w in the amplitude terms and taking into account the change of H_w in

the detuning:

$$C = \kappa_w - \omega[1 + Q_w^2(z)]/2\gamma_0^2, \qquad Q_w = eH_w(z)/mc^2\kappa_w.$$

Simulation of nonlinear mode of the FEL operation is performed by macroparticle method. When the number of macroparticles per radiation wavelength (or phase interval $0 < \psi < 2\pi$) is equal to M, the equations of motion of the k-th particle are as follows:

$$d\hat{P}_{(k)}/d\hat{z} = \hat{u}(z)\cos(\psi_{(k)} + \psi_0), \tag{B.1}$$

$$d\psi_{(k)}/d\hat{z} = \hat{P}_{(k)} + \hat{C}. \tag{B.2}$$

Here the following notations have been introduced: $\hat{z} = z/l_w$, $\hat{C} = Cl_w$, l_w is the length of the main undulator, $\hat{P} = \omega l_w P/c\gamma_{z0}^2\mathcal{E}_0$, $P = \mathcal{E} - \mathcal{E}_0$, $\hat{u} = \omega l_w^2 u/c\gamma_{z0}^2\mathcal{E}_0$, $u\exp(i\psi_0) = -e\theta_w\tilde{E}$, $\theta_w = Q_w(0)/\gamma_0$, $\gamma_0 = \mathcal{E}_0/mc^2$ and $\gamma_{z0}^{-2} = \gamma_0^{-2} + \theta_w^2$.

We assume the transverse size of the electron beam to be much less than aperture of diaphragm line, so we neglect the radiation field change in the transverse direction. Using Maxwell equation, we obtain the following reduced equations on the amplitude $\hat{u}$ and phase ψ_0 of effective potential:

$$d\hat{u}/d\hat{z} = -\frac{2\tau}{M}\sum_{k=1}^{M}\cos(\psi_{(k)} + \psi_0), \tag{B.3}$$

$$d\psi_0/d\hat{z} = \frac{2\tau}{M\hat{u}}\sum_{k=1}^{M}\sin(\psi_{(k)} + \psi_0), \tag{B.4}$$

where

$$\tau = \pi\theta_w^2 j_0 \omega l_w^3 (c\gamma_{z0}^2\gamma_0 I_A)^{-1} \tag{B.5}$$

is the gain parameter and $I_A \simeq 17$ kA. To take into account the field distribution in the diaphragm line, an effective electron current density should be substituted into the equations:

$$j_0 = I[\pi R^2 J_1^2(\mu_{01})]^{-1} \simeq 3.7I/(\pi R^2).$$

Here we have taken into account that transverse field distribution of the ground TEM_{00} mode of the axisymmetric diaphragm line is given with the expression (see Appendix A):

$$|\tilde{E}| \propto J_0(\mu_{01} r/R).$$

The solution of equations (B.2) - (B.4) allows one to obtain the field amplification $G = \Delta\hat{u}/\hat{u}$ per one undulator pass. The electron efficiency of the FEL is given with the expression:

$$\eta = ce\,|\tilde{E}\Delta\tilde{E}|/(\pi j_0\mathcal{E}_0),$$

or

$$\hat{\eta} = \eta/g = \hat{G}\hat{u}^2/2, \tag{B.6}$$

where $\hat{G} = G/\tau$ and

$$g = \gamma_{z0}^2 c/\omega l_w, \qquad g \ll 1. \tag{B.7}$$

Under accepted approximations, namely of a small gain and that there is a bunched beam at the main undulator entrance, it follows from eq. (B.2) that the main undulator should be tapered by a linear law:

$$\hat{C}(\hat{z}) = \hat{C}(0) + \hat{\alpha}\hat{z}. \tag{B.8}$$

When the undulator tapering is performed by the undulator field decrease at a fixed undulator period, the linear law of the tapering (B.8) takes place at a linear change of the undulator field along the undulator axis:

$$[H_w(z) - H_w(0)]/H_w(0) = \alpha z,$$

where α is equal to

$$\hat{\alpha} = \alpha\omega l_w Q_w^2(0)/g(1 + Q_w^2(0)).$$

To obtain simple physical estimations for the FEL efficiency, let us consider a model situation when the electron beam is totally bunched and is located in an optimal decelerating phase at the entrance of the main undulator (i.e. $M = 1$, $\psi_{(1)}(0) \simeq \pi$, $\psi_0 = 0$ in equations (B.2) - (B.4)). In this case the optimal value of the tapering parameter $\hat{\alpha}$ is equal to $\hat{\alpha} \simeq \hat{u}$ and the change of the energy, in accordance with eq. (B.2), is given with the expression $\hat{P} \simeq -\hat{u}\hat{z} \simeq -\hat{\alpha}\hat{z}$. The change of the field amplitude, in accordance with eq. (B.4), is equal to $\Delta\hat{u} \simeq 2\tau$ and the field gain is equal to $G = \Delta\hat{u}/\hat{u} \simeq 2\tau/\hat{u}$. Substituting the latter expression into formula (B.6), we obtain expression for the FEL efficiency:

$$\hat{\eta} = \eta/g \simeq \hat{u}.$$

A thorough optimization of the FEL amplifier with the multicomponent undulator, performed with a large number of macroparticles, confirms these parametric dependencies $\hat{\eta} \propto \hat{u}$, $\hat{\alpha} \propto \hat{u}$ and $\hat{G} \propto \hat{u}^{-1}$, but results in smaller coefficients, namely:

$$\hat{\eta} \simeq 0.65\hat{u}, \qquad \hat{\alpha} \simeq 0.9\hat{u}, \qquad \hat{G} \simeq 1.3\hat{u}^{-1} \tag{B.9}$$

In the real situation, the particles occupy a finite region in the phase space and perform synchrotron oscillations near the equilibrium phase $\psi_s = \arccos[-\hat{\alpha}/(\hat{u})] \simeq 2.7$. The mean value of the energy of the trapped particles is equal to $< \Delta\mathcal{E}/\mathcal{E}_0 >_{tr} = g < \hat{P} >_{tr} \simeq -g\hat{\alpha}\hat{z}$.

Let us now consider a situation when the electron efficiency, calculated with formula (B.9),

$$\eta \simeq 0.65g\hat{u},$$

is of the order of unity, which corresponds to the case of the high efficiency, i.e. a significant change of the electron energy occurs during the amplification process. In this case equations (B.2) - (B.4) should be modified to

$$\frac{d\hat{P}_{(k)}}{d\hat{z}} = \frac{1 - g\hat{\alpha}\hat{z}(1+b)/b}{1 + g\hat{P}_{(k)}}\hat{u}(z)\cos(\psi_{(k)} + \psi_0), \tag{B.10}$$

$$\frac{d\psi_{(k)}}{d\hat{z}} = \hat{C}_0 + \frac{P_{(k)}(1 + g\hat{P}_{(k)}/2) + \hat{\alpha}\hat{z}\,[1 - g\hat{\alpha}\hat{z}(1+b)/(2b)]}{(1 + g\hat{P}_{(k)})^2}, \tag{B.11}$$

$$\frac{d\hat{u}}{d\hat{z}} = -\frac{2\tau}{M}[1 - g\hat{\alpha}\hat{z}(1+b)/b]\sum_{k=1}^{M}\frac{\cos(\psi_{(k)} + \psi_0)}{1 + g\hat{P}_{(k)}}, \tag{B.12}$$

$$\frac{d\psi_0}{d\hat{z}} = \frac{2\tau}{M\hat{u}}[1 - g\hat{\alpha}\hat{z}(1+b)/b]\sum_{k=1}^{M}\frac{\sin(\psi_{(k)} + \psi_0)}{1 + g\hat{P}_{(k)}}, \tag{B.13}$$

where $b = Q_w^2(0)$. These equation are reduced in the same way as equations (B.2) - (B.4). The only difference is that all reduced parameters are calculated at the initial parameters of the electron beam and undulator. Parameters $\hat{\alpha}$ and α are connected with each other by the relation: $\hat{\alpha} = \alpha b l_w/g(1+b)$.

Reduced length of the prebuncher is equal to $\hat{l}_p = l_p/l_w$. The change of the phases of electrons in the drift space of length l_d is given with the expression:

$$\Delta\psi_{(k)} = \left[\hat{C}_0 + \hat{P}_{(k)}\right]\hat{l}_d + \delta\psi,$$

where $\hat{l}_d = l_d[1 + Q_w^2(0)]^{-1}l_w^{-1}$ and $\delta\psi = -\pi l_d/(\gamma_0^2\lambda) = -\hat{l}_d/2g$ is the phase shift due to the optical beam slippage with respect to the electron beam to be not multiple to the radiation wavelength.

When the energy spread of electrons in the beam is gaussian at the undulator entrance,

$$F(P) = \left[2\pi\sigma^2\right]^{-1/2}\exp\left[-(\mathcal{E} - \mathcal{E}_0)^2/(2\sigma^2)\right],$$

then reduced distribution of macroparticles is given with the expression:

$$\hat{F}(\hat{P}) = \left[2\pi\hat{\Lambda}_T^2\right]^{-1/2}\exp\left[-\hat{P}^2/2\hat{\Lambda}_T^2\right], \tag{B.14}$$

where $\hat{\Lambda}_T = \sigma/\mathcal{E}_0 g$ is the energy spread parameter.

So, equations (B.11) - (B.13) allow one to simulate the FEL amplifier with a high efficiency. It should be noticed that in the high-efficiency case it is rather difficult to obtain universal formulae for the efficiency similar to formulae (B.9) obtained for a low-efficiency case. In the general case, numerical simulation should be performed as soon as parameters of the FEL amplifier have been changed. Nevertheless, we can make some useful remarks.

First, at the linear law of tapering, the obtained efficiency will be lower than that given with formulae (B.9). It is connected with the fact that when efficiency approaches to unity, the size of separatrix is decreased:

$$(\delta\hat{P})_{\max} = S[(1 - g\hat{\alpha}\hat{z})\hat{u}]^{1/2}, \tag{B.15}$$

where factor S is of the order of unity. So, we may conclude that the value of the efficiency depends on the value of $g\hat{\alpha}$ (or on the value of $g\hat{u}$, because $\hat{\alpha} \propto \hat{u}$).

Another effect decreasing the FEL efficiency is the influence of the energy spread in the electron beam. To diminish this effect, we should provide the energy modulation in the prebuncher $(\delta\hat{P})_p = \hat{u}\hat{l}_p$ to be greater than the energy spread in the beam $\hat{\Lambda}_T$. On the other hand, the energy modulation in the prebuncher should be less than the size of separatrix, $(\delta\hat{P})_p < S\hat{u}^{1/2}$. So, we may conclude that the energy spread will not decrease the FEL efficiency when

$$\hat{\Lambda}_T\hat{u}^{-1/2} \ll 1.$$

Taking into account the above mentioned remarks, expression for the FEL efficiency may be written in the following form:

$$\eta \simeq 0.65g\hat{u}f(g\hat{u}, \hat{\Lambda}_T\hat{u}^{-1/2}), \tag{B.16}$$

where function f is close to unity at small values of arguments and is decreased with their growth. In the general case, when the values of $g\hat{u}$ and $\hat{\Lambda}_T\hat{u}^{-1/2}$ are rather large, it is necessary to perform optimization of all parameters of the FEL amplifier including the choice of the equilibrium decelerating phase, of the reduced length of the prebuncher $\hat{l}_p$, of the reduced length of the drift space $\hat{l}_d$ and of the phase shift in the drift space $\delta\psi$.

References

[1] Status reports on ICF laser programs can be found in:
Proceedings of the Thirteenth International Conference on Plasma Physics and Controlled Fusion Research (Washington, D.C., 1 -9 October, 1990), Vol. 3;
Proceedings of the Fourteenth International Conference on Plasma Physics and Controlled Fusion Research (Würzburg, 30 September - 7 October 1992), Vol. 3, 4

[2] S. Nakai et al., Proceedings of the Fourteenth International Conference on Plasma Physics and Controlled Fusion Research (Würzburg, 30 September - 7 October 1992), Vol. 3, p.13

[3] K. Mima et al., Proceedings of the Fourteenth International Conference on Plasma Physics and Controlled Fusion Research (Würzburg, 30 September - 7 October 1992), Vol. 3, p. 381

[4] T.J. Orzechowski et al., Phys. Rev. Lett. **57**(1986)2172

[5] K. Imasaki et al., Nucl. Instrum. and Methods **A318**(1992)20

[6] G.T. Moore, Nucl. Instrum. and Methods **A239**(1985)19

[7] C. Rubbia, CERN-PPE/92-61 (April,1992)

[8] L.A. Veinstein, Open Resonators and Wave guides (Moscow, Sovetskoye Radio, 1966)

[9] J. Duderstadt and G. Mozes, Inertial Confinement Fusion. John Willey and Sons, New York, 1982.

[10] Yu.V. Afanas'ev, N.G. Basov et al., Sov. Pis'ma v Zh. Exp. Teor. Phys., **21**(1975)150
Yu.V. Afanas'ev, N.G. Basov et al., Sov. Pis'ma v Zh. Exp. Teor. Phys., **24**(1976)23

[11] E.L. Saldin, E.A. Schneidmiller and M.V. Yurkov, Optics Communications, **97**(1993)272

[12] E.L. Saldin, E.A. Schneidmiller and M.V. Yurkov, Optics Communications, **95**(1993)141

[13] A.M. Kondratenko, E.V. Pakhtusova and E.L. Saldin, Dokl. Akad. Nauk **264**(1982)849, Preprint INF 81-130, Novosibirsk (1981), in Russian

[14] N. Kroll, P. Morton and M. Rosenbluth, SRI Rep. JSR-79-01; IEEE J. Quant. Electr. **QE-17**(1981)1436

[15] P. Sprangle, C.M. Tang and W.M. Manheimer, Phys. Rev. **A21**(1980)302

[16] D. Price et al., Proceedings of the 1989 IEEE Particle Accelerator Conference, Vol.2, p.941, Chicago, 1989

[17] K. Batchelor et al., Nucl. Instrum. and Methods **A318**(1992)372

[18] J.T. Seeman, SLAC-PUB-5607 (July, 1991), SLAC-PUB-5748 (June, 1992)

[19] D.A.G. Deacon et al., Phys. Rev. Lett. **38**(1977)892

[20] L.P. Elias and J.M.J. Madey, Rev. Sci. Instr. **50**(1979)1335

[21] H. Buchholz, Elektrische und magnetische Potetialfelder (Berlin – Göttingen – Heidelberg, Springer – Verlag, 1957)

[22] E. Minehara et al., Proceedings of the 8th Symposium on Accelerator Science and Technology (Saitama, Japan, November 25 - 27, 1991), Ionics Publishing Company, Tokyo, 1991, p. 246

[23] M. Tigner, "Proceedings of the LC'92 ECFA Workshop on e^+e^- Linear Colliders (July, 25 – August , 2, 1993, Germany)", MPI-PhE/93-14, ECFA 93-154, p. 227

[24] A.G. Fox and T. Li, Bell Syst.Tech.J. **40**(1961)453

[25] Y.A. Anan'ev, Optical Resonators and Laser beams (Moscow, Nauka, 1990)

[26] M. Born and E. Wolf, Principles of Optics (Pergamon Press, 1968)

[27] S. Solimeno, B.Crosignani, P. DiPorto, Guiding, Diffraction and Confinement of Optical Radiation (Academic Press, INC, 1986)

Салдин Е.Л. и др. E9-94-237

Лазер на свободных электронах для инерциального термоядерного синтеза

Предложена новая концепция лазера для промышленного термоядерного реактора на основе инерциального термоядерного синтеза (ИТС). Схема основана на применении лазера на свободных электронах (ЛСЭ) в качестве источника энергии для сжатия термоядерной мишени, что становится возможным благодаря применению принципиально новой схемы ЛСЭ-усилителя, предложенной в данной работе. В рассмотренном проекте лазерная система на базе ЛСЭ работает на длине волны 0,5 мкм. Полная энергия лазерного излучения равна 1 МДж. Эта энергия доставляется на мишень в импульсе с длительностью, регулируемой в пределах 0,1—2 нс. Яркость лазерной системы составляет 4×10^{22} Вт $см^{-2}$ $ср^{-1}$. ЛСЭ работает с частотой повторения импульсов 40 Гц, полная эффективность преобразования электроэнергии в энергию оптического излучения составляет 11%. Показано, что размеры и стоимость источника энергии на базе ЛСЭ сопоставимы с размерами и стоимостью соответствующего источника на основе пучков тяжелых ионов, в то время как проблемы технической реализации могут быть разрешены на современном уровне развития ускорительной техники.

Работа выполнена в Лаборатории сверхвысоких энергий ОИЯИ.

Препринт Объединенного института ядерных исследований. Дубна, 1994

Saldin E.L. et al. E9-94-237

Free Electron Laser as Energy Driver for Inertial Confinement Fusion

An FEL based energy driver for Inertial Confinement Fusion (ICF) is proposed. The key element of the scheme is free electron laser system. Novel technical solutions reveal a possibility to construct the FEL system operating at radiation wavelength $\lambda = 0.5\,\mu m$ and providing flash energy $E = 1$ MJ and brightness 4×10^{22} W cm^{-2} sr^{-1} within steering pulse duration 0.1—2 ns. Total energy efficiency of the proposed ICF energy driver is about of 11% and repetition rate is 40 Hz. Dimensions of such an ICF driver are comparable with those of heavy-ion ICF driver, while the problem of technical realization seems to be more realistic. It is shown that the FEL based ICF energy driver may be constructed at the present level of accelerator technique R&D.

The investigation has been performed at the Particle Physics Laboratory, JINR.

Preprint of the Joint Institute for Nuclear Research. Dubna, 1994